Author Manuscript

Author Manuscript

Author Manuscript

Author Manuscript

HHS Public Access

Author manuscript

*Nat Neurosci*. Author manuscript; available in PMC 2020 April 21.

Published in final edited form as:

*Nat Neurosci*. 2019 November ; 22(11): 1771–1781. doi:10.1038/s41593-019-0511-3.

# Neuronal network activity controls microglial process surveillance in awake mice via norepinephrine signaling

**Yong U. Liu**[1], **Yanlu Ying**[1], **Yujiao Li**[1], **Ukpong B. Eyo**[1,2], **Tingjun Chen**[1], **Jiaying Zheng**[1], **Anthony D. Umpierre**[1], **Jia Zhu**[1], **Dale B. Bosco**[1], **Hailong Dong**[3], **Long-Jun Wu**[1,4,5,*]

[1]Department of Neurology, Mayo Clinic, Rochester, MN 55905, USA

[2]Department of Neuroscience and Center for Brain Immunology and Glia, University of Virginia, Charlottesville, MN 22908, USA

[3]Department of Anesthesiology, Xijing Hospital, Fourth Military Medical University, Xi'an, 710032l, China.

[4]Department of Neuroscience, Mayo Clinic, Jacksonville, FL 32224, USA

[5]Department of Immunology, Mayo Clinic, Rochester, MN 55905, USA

## Abstract

Microglia dynamically survey the brain parenchyma. Microglial processes interact with neuronal elements; however, the role neuronal network activity plays in regulating microglial dynamics is not entirely clear. Most studies of microglial dynamics use either slice preparations or in vivo imaging in anesthetized mice. Here we demonstrate that microglia in awake mice have relatively reduced process area and surveillance territory, and that reduced neuronal activity under general anesthesia increases microglial process velocity, extension and territory surveillance. Similarly, reductions in local neuronal activity through sensory deprivation or optogenetic inhibition increase microglial process surveillance. Using pharmacological and chemogenetic approaches, we demonstrate that reduced norepinephrine signaling is necessary for these increases in microglial process surveillance. These findings indicate that under basal physiological conditions noradrenergic tone in awake mice suppresses microglial process surveillance. Our results emphasize the importance of awake imaging for studying microglia–neuron interactions and demonstrate how neuronal activity influences microglial process dynamics.

## Introduction

Microglia are the resident immune cells of the central nervous system (CNS) that interact with neuronal elements in the brain parenchyma[1–3]. Under normal conditions, microglia

Users may view, print, copy, and download text and data-mine the content in such documents, for the purposes of academic research, subject always to the full Conditions of use:http://www.nature.com/authors/editorial_policies/license.html#terms

[*]**Correspondence:** ***Dr. Long-Jun Wu***, Department of Neurology, Mayo Clinic, 200 First Street SW, Rochester, MN 55905, TEL: (617) 943-7822, wu.longjun@mayo.edu.

**Author Contributions:** Y.U.L., H.D., and L.J.W. designed the studies. Y.U.L., A.D.U., and L.J.W. wrote and revised the manuscript. Y.U.L. performed the electrophysiology. Y.U.L., Y.Y., Y.L., U.B.E., T.C., J.Y.Z., A.D.U., J.Z. and D.B.B. performed animal surgery, imaging collection and data analysis. Y.U.L. and J.Y.Z performed *in situ* hybridization and immunofluorescence staining.

**Conflict of Interest:** The authors declare no competing interests.

Author Manuscript Author Manuscript Author Manuscript Author Manuscript

participate in synaptic pruning during brain development as well as synaptic remodeling during learning[4, 5]. Within neurological disorders such as pain, stroke, epilepsy, autoimmune diseases, and neurodegeneration, microglia play key roles in pathology and can exert either detrimental or beneficial effects[6]. Multiple lines of evidence suggest that contact between microglial processes and neuronal dendrites can lead to changes in neuronal structure and function. Particularly during early developmental periods, microglial process contact can induce filipodia outgrowth from dendrites[7, 8]. Conversely, in later development, microglial contact results in a higher probability of spine elimination[9]. This later interaction may be a key component of synaptic pruning and neuronal circuit formation[8, 10]. In the mature brain, microglia can promote spine formation via BDNF signaling, thereby interaction with the molecular mechanisms of learning and memory[11]. In addition, microglial processes can enhance dendritic calcium activity and may influence neuronal synchrony at the population level[12]. While microglial contact can influence neuronal structure and function across the developmental lifespan, it is unclear how microglial process dynamics are regulated in the basal state, particularly in the awake animal.

As surveilling immune cells, microglia dynamically respond to changes in the microenvironment with their remarkably motile processes[13–15]. To date, most studies of microglia process dynamics have occurred in slice preparations or under the constraints of general anesthesia *in vivo*. These studies showed that following laser-induced injury, local microglia quickly respond to damage by extending processes to isolate the injury site, using an ATP/$P2Y_{12}$ signaling mechanism[13, 14, 16, 17]. In addition, suppression of the neuronal network via tetrodotoxin results in either reduced microglial-neuron contact[18] or no significant changes in microglial process surveillance[13]. Conversely, enhancements of the neuronal network via interneuron inhibition can lead to increases in process sampling[13]. Under more extreme circumstances, suprathreshold neuronal activity or acute seizure induction can further induce microglial process extension and convergence towards hyperactive neurons[19, 20]. Thus, dynamic microglial processes are able to sense brain injury and neuronal activity in basal and disease contexts. More specifically, microglial process dynamics appear to follow activity-dependent patterns in anesthetized animals.

Despite the importance of microglia process dynamics in neuronal interactions, we currently do not know how microglial processes behave under the most physiologically relevant conditions (*i.e.*, in the awake state). Using *in vivo* two-photon imaging in awake mice, we surprisingly find that microglial processes are less dynamic and survey a smaller territory before neuronal activity is suppressed by general anesthesia. In awake animals, other methods of neuronal suppression, including sensory deprivation (whisker trimming) or optogenetic inhibition mimicked the relative increase in microglial process surveillance. We found that adrenergic but not purinergic signaling controls the microglial surveillance phenotype observed in the awake state. Accordingly, in the awake state, pharmacological inhibition of β2-adrenergic receptors or chemogenetic reductions of norepinephrine (NE) release from the locus coeruleus (LC) resulted in microglial process extension and increased surveillance territory. Thus, under awake conditions, microglial processes have constrained dynamics set by tonic NE tone. Under anesthesia, loss of NE tone becomes permissive for microglia surveillance increases. Our findings in the awake animal demonstrate that microglial dynamics cannot be dictated by neuronal activity through a linear relationship.

Author Manuscript Author Manuscript Author Manuscript Author Manuscript

Instead, we advance a theory that microglial dynamics follow a "U-shape" model of dynamics in response to neuronal activity via noradrenergic signaling.

## Results

### Microglial process surveillance increases after general anesthesia

Microglia processes extend and retract to survey the brain parenchyma. We first investigated how microglial process dynamics behave in the awake state using CX3CR1$^{GFP/+}$ mice to visualize microglia in the somatosensory cortex (Supplementary Fig. 1a–d). After recovery from cranial window surgery (2–4 weeks), mice were trained to freely move on a custom-made, rotating treadmill while head restrained (Supplementary Fig. 1a). Using *in vivo* two-photon imaging, we observed that microglial processes maintain a relatively stable territory of surveillance in awake animals (Supplementary Fig. 1e–g).

We initially hypothesized that microglia process surveillance is neuronal activity dependent, and would therefore be attenuated by general anesthesia. However, when isoflurane (1.2% in oxygen, 700 mL/min) was applied to the animal via a nose cone, we surprisingly observed that microglial processes began to extend and occupy a greater area of brain parenchyma, herein termed process surveillance (Fig. 1a, b; Supplementary Movie 1). Increased process surveillance was initiated a few minutes after isoflurane induction and reached peak levels after 20 to 30 minutes. As expected, neuronal network activity in the cortex was strongly suppressed immediately after isoflurane induction, as determined by dampened calcium spikes in GCaMP6s-expressing cortical neurons (Fig. 1a, b; Supplementary Fig. 2a–d and Movie 2) and by *in vivo* electrophysiology showing slow wave activity (Supplementary Fig. 2e–f). We found that 10 minutes of isoflurane administration is sufficient to initiate an increase in microglial process surveillance that persists for at least 50 minutes after isoflurane cessation (Supplementary Fig. 3). Thus, increases in microglial process surveillance represent a delayed but persistent response to the suppression of cortical network activity. Accompanying their increased process surveillance, microglia also exhibited faster process movement velocity (Fig. 1c) and more intricate ramified morphology, as demonstrated by Sholl analysis, process length, and number of branch points (Fig. 1e–g). These results reveal that isoflurane anesthesia enhances rather than inhibits microglial process dynamics.

Among other targets, isoflurane can inhibit the microglial two-pore domain potassium channel THIK-1, which controls microglial process ramification and surveillance[21]. Our results however showed that isoflurane increases rather than decreases microglial process surveillance. Therefore, to determine whether the microglial process surveillance changes were unique to isoflurane administration or represented a broader microglial response to general anesthesia, we also investigated the effects of two other commonly used anesthetics, ketamine/xylazine and urethane. Similar to isoflurane inhalation, systemic administration (i.p.) of either ketamine/xylazine (87.5 mg/kg Ket, 12.5 mg/kg Xy) or urethane (1.6 g/kg) increased microglia process surveillance (Fig. 1h, i). Thus, multiple classes of general anesthetics can enhance microglial process surveillance relative to the awake state. Our results suggest that the awake condition may represent a constrained state of microglia in surveying the brain parenchyma.

Author Manuscript Author Manuscript Author Manuscript Author Manuscript

To further delineate the potential function of microglial process surveillance, we performed two lines of experiments: (1) microglial process chemotaxis towards laser injury, and (2) microglial process interaction with neuronal dendrites. We found that the velocity of microglial process chemotaxis in response to laser burn was significantly higher under anesthesia than in the awake condition (Supplementary Fig. 4a). Next, we used CX3CR1$^{GFP/+}$:Thy1-YFP mice to examine microglial process interaction with neuronal dendrites *in vivo*. We found that microglial processes displayed longer contact duration and a larger contact area with dendrites under anesthesia compared to the awake condition (Supplementary Fig. 4b, c). These latter results suggest that increased microglial process surveillance could be translated into enhanced microglia-neuron interaction under anesthesia.

## Whisker trimming increases microglial process surveillance in awake mice

Suppressed neuronal activity precedes the increase in microglial process surveillance under general anesthesia, suggesting that neuronal activity may negatively regulate microglial process dynamics. However, general anesthesia also alters metabolism, blood pressure, and cardiac output[22]. For these reasons, we additionally employed unilateral whisker trimming as an approach to reduce neuronal activity and study microglial process dynamics[23]. Whisker trimming is a sensory deprivation method that suppresses neuronal activity in the contralateral barrel cortex, demonstrated by calcium imaging in GCaMP6s-expressing cortical neurons (Supplementary Fig. 5a–c and Movie 3). In response to whisker trimming, microglia in the contralateral barrel cortex began to increase their process area and survey a greater territory of barrel cortex, similar to the findings induced by general anesthesia (Fig. 2a, b; Supplementary Movie 4). Moreover, the latency for microglia to increase their surveillance after whisker trimming has a similar slow onset time course when compared to anesthesia (Supplementary Fig. 5d, e). Sensory deprivation only increased process surveillance in microglia of the contralateral barrel cortex, with no effect observed for microglia of the ipsilateral barrel cortex (Fig. 2c, d). Therefore, these results demonstrate that reductions in region-specific sensory input selectively and negatively regulates microglial process surveillance.

Our whisker trimming experiments further substantiate the observation that reduced neuronal activity enhances microglial process surveillance. To determine whether sensory deprivation and general anesthesia increase microglial process surveillance through unique or shared mechanisms, we determined whether their combination had an additive effect on microglial surveillance. To this end, we performed unilateral whisker trimming followed by isoflurane inhalation after an additional 30 min. We found that whisker trimming increased microglial process surveillance, but the addition of isoflurane anesthesia could not further increase process surveillance (Fig. 2e, f). Thus, whisker trimming and isoflurane anesthesia do not have additive effects on microglia process surveillance, suggesting they may share a similar mechanism for triggering an increase in microglial process dynamics.

Author Manuscript Author Manuscript Author Manuscript Author Manuscript

## Both pharmacological and optogenetic inhibition of neuronal network activity increases microglial process surveillance in awake mice

Results from general anesthesia and sensory deprivation indicate that neuronal activity regulates microglial process dynamics. To directly test this idea, we manipulated cortical network activity through pharmacological and optogenetic approaches and then examined microglial process surveillance. We used an intracerebral catheter and applied a potent and selective agonist for $GABA_A$ receptors, muscimol (870 μM, 10 μL), to suppress neuronal network activity in the somatosensory cortex (Fig. 3a). Indeed, we found that muscimol application in awake mice reduced neuronal calcium activity in the somatosensory cortex (Supplementary Fig. 6 and Movie 5). Coincident with the reduction in neuronal calcium activity, microglia increased their process surveillance (Fig. 3a, c; Supplementary Movie 6). By contrast, intracerebral application of ACSF did not alter microglial process surveillance (Fig. 3b). Similarly, we found that microglial surveillance increases after intracerebral application of tetrodotoxin (TTX, 10 μM) to inhibit neuronal firing in the awake animal (Supplementary Fig. 7). Thus, pharmacological inhibition of local neuronal network activity in the cortex is able to recapitulate changes in microglial process dynamics under general anesthesia or whisker trimming.

Next, we employed an optogenetic strategy to suppress neuronal activity. Channelrhodopsin 2 (ChR2) was expressed in VGAT-positive GABAergic neuron populations using VGAT-ChR2 transgenic mice. Optogenetic activation of GABAergic cell populations in this transgenic line has been previously shown to suppress neuronal network activity[24]. Proper ChR2 expression and function in VGAT-positive interneurons was confirmed in our experiments by whole-cell patch clamp recording in acute brain slices (Fig. 4a, b; Supplementary Fig. 8a, b). We found that in awake mice, activation of VGAT-ChR2 by 470 nm blue light (10 Hz, 10 min) increased microglial process surveillance (Fig. 4c, d; Supplementary Movie 7 and Fig. 8c, d). Building upon findings during general anesthesia (Supplementary Fig. 3), transient and reversible network inhibition via optogenetic methods could trigger a prolonged increase in microglial surveillance, sustained for at least 20 min (Supplementary Fig. 8c, d). Together, these results demonstrate that inhibition of local cortical network activity by pharmacological or optogenetic means can trigger an increase in microglial process surveillance in awake mice.

## Norepinephrine signaling regulates microglial process surveillance in awake mice

Next, we investigated the molecular mechanisms underlying the observed increase in microglial process surveillance following neuronal activity suppression. To date, the ATP/ADP-sensing $P2Y_{12}$ receptor has been shown to regulate microglial process extension in a variety of contexts[14, 20, 25]. To test whether $P2Y_{12}$ signaling mediates the observed increase in microglial process surveillance, we imaged process surveillance in $P2Y_{12}$ deficient mice ($CX3CR1^{GFP/+}$:$P2Y_{12}^{-/-}$). Surprisingly, we found that in $P2Y_{12}^{-/-}$ mice, isoflurane anesthesia still increased microglial process surveillance (Fig. 5a, b). Therefore, unlike injury or hyperactivity-induced microglial process extension[20, 26], the observed increase in microglial surveillance is not regulated by $P2Y_{12}$ signaling. Fractalkine signaling and its receptor CX3CR1 are reported to promote microglial process dynamics and microglia-neuron interaction[27, 28]. Therefore, we then tested whether CX3CR1 contributes to the

Author Manuscript Author Manuscript Author Manuscript Author Manuscript

anesthesia-induced microglial surveillance increases by using CX3CR1$^{-/-}$ (CX3CR1$^{GFP/GFP}$) mice. We found that the administration of isoflurane anesthesia in CX3CR1$^{-/-}$ mice similarly increased microglial process surveillance (Fig. 5c, d), suggesting that fractalkine signaling is not involved in increasing microglial surveillance following anesthesia.

Previous studies have found that primary neurotransmitters such as glutamate and GABA cannot directly induce microglial process chemotaxis[20, 29]. For these reasons, we focused instead on investigating whether the neurotransmitters acetylcholine, dopamine, norepinephrine (NE), or serotonin impacted microglial process dynamics. These neurotransmitters were specifically studied because their activity is significantly decreased by general anesthesia[30]. We intracerebrally applied each neurotransmitter during isoflurane inhalation (Fig. 5e). Interestingly, we found that NE (3 mM, 10 μL) application, but not acetylcholine (5 mM, 10 μL), dopamine (1 mM, 10 μL), or serotonin (5 mM, 10 μL), was able to prevent the increase in microglial process surveillance induced by isoflurane anesthesia (Fig. 5f). These results suggest that reduced NE signaling in anesthetized condition could selectively increase microglial process surveillance.

We further studied the regulation of microglial process surveillance by NE during whisker trimming and optogenetic inhibition (Fig. 6). Intracerebral NE administration, but not ACSF administration, prevented the increase in microglial process surveillance induced contralateral whisker trimming (Fig. 6a–c). Intracerebral NE administration also prevented the increase in microglial process surveillance induced by optogenetic inhibition (Fig. 6d–f).

## β2-adrenergic receptors control microglial process surveillance in awake mice

Microglia are known to highly express β2-adrenergic receptors[31]. Their activation induces microglial process retraction in brain slices[32]. Using RNAscope *in situ* hybridization, we indeed found that most Iba1 positive microglia (97.6%) are colocalized with β2-adrenergic receptors mRNA (Supplementary Fig. 9). To explore whether adrenergic receptors control microglial process activity in awake mice, we examined the effects of β-adrenergic receptor antagonists on microglial dynamics (Fig. 7a–c). Interestingly, both the β1/β2-preferring antagonist, propranolol (300 μM, 10 μL, Fig. 7b), and the highly-selective β2 antagonist, ICI 118,551 (30 μM, 10 μL, Fig. 7c), induced an increase in microglial process surveillance in awake mice. In addition, we did intracerebral injection of TTX (50 μM) and followed by ICI 118,551 (10 μM). We found that ICI 118,551 (applied 30 min after TTX) did not further increase microglial surveillance (Supplementary Fig. 7). Thus, inhibition of β2-adrenergic receptors can increase microglial process dynamics.

Cortical NE tone is largely generated by noradrenergic neurons in the LC[33], which project into somatosensory cortex (Fig. 7d, and Supplementary Movie 8). Microglial processes are in close proximity with noradrenergic axons, labeled by AAVs (a combination of AAV.rTH.Cre and AAV.FLEX.tdTomato; Fig. 7d). To directly study the effect of NE signaling on microglia, we used a chemogenetic approach to selectively suppress noradrenergic neurons in the LC. An inhibitory Gi DREADD mouse (R26-LSL-Gi-DREADD) was bred with the CX3CR1$^{GFP/+}$ line. Expression of the Gi-DREADD receptor was confined to the LC through a targeted AAV-Cre injection (AAV9.rTH.PI.Cre.SV40)

Author Manuscript Author Manuscript Author Manuscript Author Manuscript

(Fig. 7e). In awake mice, the systemic application of CNO (5 mg/kg, i.p.) could increase microglia process surveillance in the somatosensory cortex in Gi-DREADD expressing mice but not in their control littermates (Fig. 7f–h). We confirmed that the DREADD ligand, clozapine-*N*-oxide (CNO), reduced the firing rate of Gi-DREADD expressing noradrenergic neurons in LC using acute brain slices (Supplementary Fig. 10a–d). In addition, to test potential off-target effects of CNO, we applied CNO in anesthetized Gi-DREADD mice and examined microglial process dynamics. We found that CNO did not further increase microglial surveillance in the anesthetized state (Supplementary Fig. 10e). Therefore, our results suggest that CNO targets Gi-DREDD to reduce endogenous NE release and subsequently increase microglial process surveillance.

To better access and mechanistically study LC-cortex circuitry, we performed several lines of experiments in acute cortical slices. Noradrenergic projections were well preserved (Supplementary Fig. 11a) when noradrenergic neuronal soma was severed during slice preparation (see Methods). However, unlike that shown *in vivo* (Supplementary Movie 2), neuronal network activity was weak in cortical slices (Supplementary Fig.11b, c and Movie 9). Bath application of a moderate dose of glutamate (50 μM) increased neuronal activity in cortical slices (Supplementary Fig. 11b, c and Movie 9), which resulted in reduced microglial surveillance (Fig. 8a). We further found that the β2-adrenergic receptor antagonist ICI 118,551 (10 μM) could block the glutamate-induced decreases in microglial surveillance (Fig. 8b). Next, to test the direct effect of NE on microglial dynamics in cortical brain slices, we applied exogenous NE or chemogenetically induced endogenous NE release. Indeed, we found that the exogenous application of NE (30 μM) inhibited microglial process surveillance in cortical slices; the effect was abolished by ICI 118,551 (10 μM) (Fig. 8c). The application of ICI 118,551 (10 μM) alone did not affect microglia process surveillance, presumably due to the little activity of NE-releasing axons in brain slices (Fig. 8c). In slices prepared from mice virally expressing Gq-DREADD in LC adrenergic neurons and their projections, CNO was confirmed to increase neuronal firing (Fig. 8d, e). In addition, activation of noradrenergic terminals by CNO reduced microglial process surveillance (Fig. 8f). Therefore, our results suggest that local neuronal activity can impact NE signaling, which is sufficient to regulate microglial process surveillance, even in the absence of LC somata.

Together, both β2-adrenergic receptor antagonism and chemogenetic inhibition of NE release can increase microglial process surveillance in awake mice. Inhibiting NE signaling therefore mirrors the effects of general anesthesia, sensory deprivation, and optogenetic inhibition on microglial process surveillance. Therefore, our results demonstrate that reduced NE signaling establishes a permissive microenvironment for enhanced microglial process surveillance. On the other hand, tonic NE levels in awake animals repress process surveillance and maintain a highly constrained microglial surveying state (Supplementary Fig. 12).

## Discussion

Microglia are the immune surveilling cells of the brain that shape neuronal circuitry in both health and disease[6]. Multiple studies demonstrate that the interactions between microglial

Author Manuscript Author Manuscript Author Manuscript Author Manuscript

processes and neuronal elements play a critical role in maintaining brain homeostasis[9, 18]. However, microglial process dynamics *in vivo* have been studied predominantly under anesthesia. Moreover, it is unclear whether neuronal network activity under awake conditions drive distinct microglial dynamics. Here, using *in vivo* imaging in awake mice, we show that general anesthesia, sensory deprivation, and optogenetic inhibition of local neuronal activity dramatically increases microglial process surveillance. We also pinpoint the underlying mechanism involved in increased process surveillance arises from a reduction in norepinephrine signaling to microglial β2-adrenergic receptors. These results demonstrate that neuronal network activity inhibits microglial process dynamics through tonic norepinephrine signaling in awake mice.

## Neuronal activity dictates microglial process dynamics

Prior studies of microglial imaging under anesthesia or brain slices found that microglial process dynamics seem follow neuronal activity patterns. Increased neuronal activity after bicuculline application, a $GABA_A$ receptor antagonist, enhances microglial process sampling[13]. In addition, neuronal hyperactivity triggered by NMDA receptor activation induces microglial process extension towards neuronal cell bodies and dendrites[20, 26]. Consistently, acute seizures increase microglial process dynamics and process convergence towards neuronal elements[20, 28]. During neuronal hyperactivity (*e.g.*, under seizure condition), microglia can sense ATP release via the $P2Y_{12}$ receptor and extend and converge their process towards an ATP source[20, 26].

We expected that microglia in the awake animal would display more pronounced motility. Surprisingly, we found opposite results, showing that microglia exhibit less process surveillance in the awake condition than that under general anesthesia. Consistently, introducing sensory deprivation or increased GABAergic network inhibition in awake animals resulted in similar increases in microglial process dynamics. Supporting this novel observation, a recent study reported that monocular deprivation induced greater microglial process ramification in the contralateral visual cortex[34]. Together, our results reveal that neuronal activity negatively regulates microglial surveillance in awake mice. Therefore, in awake mice, microglia process dynamics are kept in a relatively constrained state.

Our results, in combination with previous studies performed under general anesthesia, suggest that microglial process dynamics are not linearly dependent on neuronal activity (i.e. increasing neuronal activity increases microglial process dynamics). Rather, microglial dynamics follows a “U-shaped” curve of regulation, that is, either increasing or decreasing neuronal activity relative to the awake state can increase microglial process dynamics. While microglial extension and convergence during hyperactivity or acute injury has been demonstrated through an ADP/ATP and $P2Y_{12}$ dependent mechanism, we show here that a reduction in NE tone and β2-adrenergic activation (due to suppressed neuronal activity) results in microglial extension and territory surveillance. Although our results ruled out the contribution of $P2Y_{12}$ signaling in the increased territory surveillance, other studies have demonstrated that microglial $P12Y_{12}$ and β2-adrenergic receptors control microglial process motility *in vitro* through interacting mechanisms[32]. Overall, our study continues to demonstrate that microglia dynamics are highly attuned to changes in the local

Author Manuscript Author Manuscript Author Manuscript Author Manuscript

microenvironment, but follow a "U-shape" style of regulation rather than linear activity dependent regulation.

## Tonic norepinephrine and microglial process dynamics

Here we demonstrate that tonic norepinephrine signaling selectively regulates microglial process surveillance *in vivo* based on several lines of evidence. First, of the four potential neuromodulators tested (Ach, DA, NE, and 5-HT), only NE was able to prevent anesthesia-induced microglia process extension. Second, exogenous NE also prevented the increase of microglial process surveillance induced by whisker-trimming and optogenetic inhibition. Finally, pharmacological inhibition of microglial β2-adrenergic receptors and chemogenetic inhibition of LC noradrenergic neuron increased microglial process surveillance in awake mice. LC noradrenergic neurons are the exclusive source of NE in the cortex[35]. Indeed, we show abundant LC projections in the somatosensory cortex, consistent with the reported ~1.2 million axon varicosities per LC neuron[36]. Additionally, a wealth of adrenergic receptors are expressed in neurons and glia[37]. Among them, the β2-adrenergic receptor is highly enriched in microglia when compared to other cell types[31]. Previous studies have also shown that microglial β2-adrenergic receptors are critical for microglial motility, migration, phagocytosis, proliferation, and inflammatory responses[37]. Our study corroborates the importance of noradrenergic regulation of microglia function by providing the first evidence that tonic NE inhibits microglial process surveillance via β2-adrenergic receptors in awake mice.

While microglia represent an enriched cell population for functional β2-adrenergic receptor expression[31], the downstream signaling cascades that mediate β2-dependent process motility and surveillance are still undefined in microglia. It is known that the β2-adrenergic receptor is coupled to Gs protein signaling. Thus, inhibition of microglial β2 receptors should reduce cAMP production, based upon canonical Gs signaling[38]. Similarly, the Gi-coupled $P2Y_{12}$ receptor, which also alters cAMP levels, induces microglial process chemotaxis, while the Gs-coupled $A_{2A}$ receptor mediates microglial process retraction[39]. Therefore, it seems that the intracellular cAMP level is important in regulating microglial process surveillance. Indeed, a very recent study demonstrated that cAMP controls microglial filopodia dynamics[40]. However, future studies on whether and how cAMP levels drive microglial process surveillance *in vivo* are still needed.

Our findings strike an interesting contrast to recent work investigating the impact of halogenated anesthetics, such as isoflurane, on microglial process dynamics. Tonic activation of the microglial two-pore domain channel THIK-1 was recently shown to control microglial process ramification and surveillance[21]. THIK-1 inhibition via isoflurane is able to reduce microglial process surveillance in hippocampal slices. In contrast, our study indicates that isoflurane increases microglial process dynamics in the cortex of awake mice. This discrepancy could be due to microglial heterogeneity within different brain regions (hippocampus vs. cortex), but could also be explained by the expected attenuation of NE tone that occurs when LC projections are severed during brain slice preparation. In brain slices, microglial surveillance is likely to be elevated in the absence of a strong NE tone. Potentially when microglia are relieved of the dynamic constraints set by NE tone in slices,

Author Manuscript Author Manuscript Author Manuscript Author Manuscript

they are disposed to greater modulation in the microenvironment. *In vivo*, it is possible that the effects of isoflurane on NE tone serve as a stronger impetus for altering microglial dynamics than the effects of isoflurane on THIK-1 signaling. However, studies directly assessing β2 and THIK-1 signaling on microglial process surveillance will be necessary to clearly understand the conditions and constraints for their functions.

## Functional significance of microglia process dynamics regulated by norepinephrine tone

Increased microglial process surveillance broadly suggests more interactions between microglia and features of the brain parenchyma, such as neurons and vasculature[7, 41, 42]. The functional significance of microglial process interaction with neurons is an emerging field of research. Previous studies indicate that microglial interaction may dampen neuronal hyperactivity[20, 43], while other studies show that microglial processes increase dendritic spine $Ca^{2+}$ activity[12] and promote new spine formation during brain development and learning[7, 11]. Therefore, microglial process surveillance may play a beneficial role in fine-tuning neuronal activity, by reducing neuronal activity during seizures[19, 20], or increasing neuronal synchronization during periods of reduced network activity[12]. Calibrating neuronal activity occurs in response to divergent neuromodulatory signals that exist in various brain states. While distinct receptors (*i.e.*, $P2Y_{12}$, β2) for these divergent neuromodulators have been identified in microglia, many more receptors are likely to exist and may aid in uniquely tuning microglial responses to the environment[3]. Towards this end, emerging tools to study intracellular signaling mechanisms, such as cAMP levels, *in vivo* may greatly advance our ability to understand the complex downstream signaling mechanisms that mediate microglial responses to the microenvironment.

LC noradrenergic neurons innervate almost every region of the brain and could therefore have a widespread, potentially uniform, impact on microglial function. Under physiological conditions, NE regulates the sleep-wake cycle in addition to its role in memory and cognition[35]. The loss of LC neurons is an early hallmark of neurodegeneration, evident in Alzheimer's disease and Parkinson's disease[44]. On the other hand, chronic stress increases LC neuronal firing rates and brain NE concentrations[45]. Therefore, the relative loss or gain in NE tone under these different pathophysiological contexts could serve as a powerful upstream modulator of microglial function across numerous brain regions. In turn, corresponding changes in microglial surveillance could produce profound consequences for the neuronal network over time in chronic conditions, based upon the described roles for microglia in tuning neuronal activity. In addition, NE has been shown to reduce pro-inflammatory gene expression in microglia in various neurological disorders including stroke, pain, and neurodegeneration[37]. Particularly, NE can help resolve pathology in mouse models of AD by promoting microglial phagocytosis of Aβ and reducing Aβ-triggered inflammation[46, 47]. However, microglia are also reported to be inappropriately activated in AD and mediate early synapse loss[48]. Apart from disease contexts, NE tone is reduced on a daily basis during sleep[49]. It would be interesting to know whether reduced NE tone during sleep may "disinhibit" microglial motility allowing greater synaptic remodeling to occur during sleep cycles, with implications for the consolidation phase of learning and memory. However, we acknowledge that anesthesia and sleep are not mechanistically identical[50], and microglial dynamics during sleep will need to be explored in greater detail in future studies.

Author Manuscript Author Manuscript Author Manuscript Author Manuscript

Additionally, even with training, head-fixed animals can still remain stressed, potentially exaggerating the levels of NE in the awake state. Therefore, for normal animals that are awake but not head-fixed, microglial surveillance could be more pronounced than we report here. Nevertheless, future studies are warranted to test the specific role of microglial adrenergic receptor signaling in sleep, memory, and neurodegeneration.

In sum, we provide novel insights of microglia process dynamics under awake conditions and their regulation by neuronal activity and NE tone. Our results demonstrate that microglial process dynamics are fundamentally different in awake animals, emphasizing the importance of studying microglia in awake mice to establish the clearest picture for their basal physiology.

## Materials and Methods

### Animals

Male and female mice, 2 to 3 months of age, were used in accordance with institutional guidelines. All experiments were approved by the Mayo Clinic Animal Care and Use Committee. Heterozygous ($CX3CR1^{GFP/+}$) mice expressing GFP under the control of the fractalkine receptor (CX3CR1) were used for all experiments[51]. $P2Y_{12}{}^{-/-}$ mice were originally donated by Dr. Michael Dailey at the University of Iowa (Iowa City, IA, USA). Heterozygous R26-LSL-Gi-DREADD mice ("Gi DREADD," Jax #026219), transgenic VGAT-ChR2 (Jax #014548) mice, and R26-LSL-tdTomato reporter mice ("td-Tomato", Jax #007909) were purchased from the Jackson Laboratory (ME, USA). Heterozygous Gi-DREADD mice were bred to homozygous $CX3CR1^{GFP/GFP}$ mice to obtain Gi-DREADD positive and negative (sibling "Control") offspring for experiments. Transgenic VGAT-ChR2 mice were also bred to homozygous $CX3CR1^{GFP/GFP}$ mice to obtain offspring with ("TG") and without ("non-TG" control) transgene expression. Finally, $P2Y_{12}{}^{-/-}$ mice were bred to $P2Y_{12}{}^{-/-}$: $CX3CR1^{GFP/GFP}$ mice to obtain $P2Y_{12}{}^{-/-}$: $CX3CR1^{GFP/+}$ animals for imaging studies. Thy1-YFP mice (Jax #003782) were bred to $CX3CR1^{GFP/GFP}$ to obtain Thy1-YFP: $CX3CR1^{GFP/+}$ in order to observe physical interaction between microglial processes and neuronal dendrites. Animals used for all experiments were randomly selected.

**Virus Injection—**To image neuronal network activity *in vivo*, 0.3 μl of AAV9.CamKII.GCaMP6s (#G12289, Penn Vector Core, PA, USA) was injected into the somatosensory cortex (2 mm posterior and 1.5 mm lateral to bregma) or barrel cortex (1.45 mm posterior and 3 mm lateral to bregma). To specifically target noradrenergic neurons, 0.3 μl of AAV9.rTH. Cre (#G12845, Penn Vector Core, PA, USA) was injected into the LC (5.4 mm posterior, 0.9 mm lateral and 3.7 mm ventral to bregma) of Gi-DREADD or td-Tomato mice bred with CX3CR1-GFP. To express Gq-DREADD in noradrenergic neurons, we injected a cocktail of three viruses: AA9.rTH.PI.Cre, AAV9.DIO.hM3D(Gq) (#44361, Addgene, MA, USA) and AAV9.FLEX.tdTomato (#28306, Addgene, MA, USA), into the LC of $CX3CR1^{GFP/+}$ mice.

**Chronic Window Implantation—**Mice were implanted with a chronic cranial window as previously described[15]. Briefly, mice were anesthetized with isoflurane (3% induction, 1.2% maintenance) and maintained on a heating pad during surgery. A dental drill (Osada Model

Author Manuscript Author Manuscript Author Manuscript Author Manuscript

EXL-M40) was used to drill a circular >3 mm diameter craniotomy. For the limb/trunk region of the somatosensory cortex, the craniotomy center was approximately 2 mm posterior and 1.5 mm lateral to bregma. For the barrel cortex, the craniotomy center was approximately −1.45 mm posterior and ± 3 mm lateral to bregma. A 3 mm glass coverslip previously sterilized in 70% ethanol was placed inside the craniotomy, then light-curing dental cement (Tetric EvoFlow) was applied around the glass coverslip and cured with a Kerr Demi Ultra LED Curing Light (Dental Health Products). The skull, excluding the region with the window, was then covered with IBond Total Etch glue (Heraeus) and cured with LED light. Finally, a custom-made head bar was attached to the skull using light-curing dental glue. Mice were allowed to recover from anesthesia on a heating pad for 10 min before they were returned to their home cage. Ibuprofen in drinking water was provided as an analgesic for 48 hours post-surgery.

***In Vivo* Two-Photon Imaging—**After recovery from cranial window surgery (2–4 weeks), mice were trained to freely move on a custom-made, rotating treadmill while head restrained (Supplementary Fig. 1a, b) for 3 days (2 sessions/day, 10 min/session). On the day of imaging, all mice with a clear, chronic glass window were included, while approximately 50% of mice with attenuated window quality were excluded prior to any data collection. Mice were imaged using a two-photon imaging system (Scientifica, UK) equipped with a tunable Ti:Sapphire Mai Tai DeepSee laser (Spectra Physics, CA, USA). Laser wavelength was tuned to 900 nm to image CX3CR1$^{GFP/+}$ microglia, 920 nm to image GCaMP6s 2fluorescence, or 950 nm to image tdTomato-labelled LC projections. Imaging utilized a 40× water-immersion lens and a 180×180 μm field of view (512×512 pixel resolution). The microscope was equipped with a 565-nm dichroic mirror and the following emission filters: 525/50 nm (green channel) and 620/60 nm (red channel) for GFP/ tdTomato imaging and a 509-nm dichroic mirror with 500/15 nm (green channel) and 537/26 nm (red channel) emission filters for GFP/YFP imaging. The laser power was maintained at 30–40 mW. Imaging in cortex was conducted 50 to 150 μm beneath the pial surface. To induce general anesthesia in awake mice, isoflurane (3% for initiation, 1.2% for maintenance) was introduced through an anesthesia nose cone. Ketamine/xylazine (87.5 mg/kg Ket, 12.5 mg/kg Xy) and urethane (1.6 mg/kg) were administered through intraperitoneal injection. The body temperature of anesthetized mice was maintained at 37 °C by a heating pad. To image microglial dynamics, we acquired z-stack images (8 sections, 2-μm step size) once every minute (Supplementary Fig. 1c). When selecting the z-stack area, we focused upon areas of cortex in which approximately three microglial somas resided at a consistent z level and had processes that could be incorporated in the x/y imaging plane. The z-stack range was then set so that microglial somas represented the approximate center of the z-range. All microglia pre-selected by these unbiased criteria were then analyzed. For calcium imaging, continuous acquisition (1 Hz time series) was carried out approximately 60 μm from the pial surface to study neuronal process calcium activity in layer 1, or approximately 150 μm from the pial surface to study neuronal soma calcium activity in layer 2/3. For laser injury, we focused the laser at 66× magnification and held it at ~250 mW for 1 s at an 800 nm wavelength. For imaging microglia-neuron interaction, we used a GFP/YFP filter set and the same acquisition protocol as microglial surveillance studies. Data collection was not performed blind to the conditions of the experiments.

Author Manuscript Author Manuscript Author Manuscript Author Manuscript

**Drug Application *in vivo*—**Intracerebral administration of neurotransmitters or antagonists was carried out through a catheter implanted 2 weeks after the chronic window implantation surgery (Fig. 3a, left panel). The catheter was carefully placed in the subarachnoid space through the cisterna magna and close to the imaging window. We verified that a dye can defuse through the catheter to the imaging window within seconds of infusion. The catheter was filled with ACSF to maintain patency and no microglia activation was observed within the area of the window after implantation. A 10 μl total solution volume was applied through the catheter and into the brain. Neurotransmitters were exogenously applied at the following concentrations: 5 mM acetylcholine chloride, 1 mM dopamine hydrochloride, 3 mM norepinephrine, 5 mM serotonin hydrochloride. The dose of muscimol (870 μM) and Tetrodotoxin (TTX, 10 μM) represents the minimal dose needed to induce significant suppression of neuronal activity. Clozapine N-oxide (CNO) was intraperitoneally injected at 5 mg/kg to activate Gi-DREADD in awake mice.

**Imaging Data Analysis—**Images were analyzed using ImageJ[52]. All microglia pre-selected by unbiased inclusion criteria were then analyzed. Inclusion criteria include a clearly identifiable soma near the center of the z stack and multiple processes incorporated within the x/y imaging plane. Because rapid movements by the animal could lead to image distortion in the x/y plane, five images were sequentially acquired at each z level (Supplementary Fig. 1c). At each z level, the user selected the image with the least distortion for inclusion in "sorted" z-stack (Supplementary Fig. 1d). Images in this z stack were then aligned along the z-axis using the StackReg plugin to create a final z-stack used in analyses.

To obtain the total process area value, a maximum-intensity projection (MIP) along the z axis was then created from the final z-stack. After applying a uniform threshold to the MIP images, the analyze particles tool was used to derive a process area value from this flattened image. To obtain a process surveillance territory value, a bounding box connecting the distal-most edges of the microglial processes was then mapped onto the MIP image. The area encompassed within this bounding box was defined as the microglial surveillance territory. Area and territory values in subsequent stacks were normalized to the values of the first stack to determine changes over time. Process velocity was measured using the "Manual tracking" plugin. Sholl analysis was performed in ImageJ with the Sholl analysis plugin. Z stacks acquired between the 10–20 min mark were used to evaluate microglial dynamics in the awake condition. Z stacks acquired between the 20–30 min mark after anesthesia (isoflurane, ketamine/xylazine, and urethane) were used to evaluate microglial dynamics in the anesthetized conditions. Similarly, z stacks acquired between the 20–30 min mark were also used for analyses following all other manipulations: pharmacological, chemogenetic, optogenetic, or sensory deprivation. For evaluating neuronal activity, calcium values above a set threshold ($\Delta F/F>0.2$) were summated in one-minute bins and reported as the normalized change in sum relative to the first minute (Fig. 1; Supplementary Fig. 3). Alternatively, the same value was summated across a 10-min period prior to and after either whisker trimming (Supplementary Fig. 5a–c), or muscimol administration (Supplementary Fig. 6).

To analyze interactions between microglial processes and neuronal dendrites, we calculated physical contact duration and the area of contact once per minute throughout a 30 min recording in the awake animal. Under anesthesia conditions, we performed identical

Author Manuscript Author Manuscript Author Manuscript Author Manuscript

measurements between 30–60 minutes after anesthesia. Contact area between microglial processes and dendrites, was normalized to the mean area of overlap determined during the first 10 min of recording in the awake condition. Data analysis was performed blind to the conditions of the experiments.

**Electrophysiology—**For verification of channelrhodopsin-2 function in VGAT-positive neurons or Gi-DREADD function in noradrenergic neurons, we studied single-cell activity in transverse, acute brain slices (350 μm) containing either somatosensory cortex (VGAT-ChR2 mice) or LC (Gi/Gq-DREADD expressed mice). Transverse or sagittal brain slices were cut in chilled (2–4 ℃) cutting solution containing (in mM): 185 sucrose, 2.5 KCl, 1.2 $NaH_2PO_4$, 25 $NaHCO_3$, 25 glucose, 10 $MgCl_2$, 0.5 $CaCl_2$. Slices were then transferred to an incubator with artificial cerebrospinal fluid (ACSF, in mM): 130 NaCl, 2.5 KCl, 1.3 $NaH_2PO_4$, 26 $NaHCO_3$, 10 glucose, 2 $MgCl_2$, 2 $CaCl_2$ (pH: 7.3–7.4; osmolarity: 300–310 mOsm; saturated with 95% $O_2$/5% $CO_2$ to provide stable pH and continuous oxygenation). For recovery, slices were kept at 29–30 °C for a 30 min period, then cooled and kept at room temperature for at least 1 hour prior to recording. During recording, slices were continuously perfused with room temperature ACSF using a peristaltic bath perfusion system. Whole-cell recordings were performed using glass pipettes (3–5 MΩ) filled with the following intracellular solution (in mM): 121 KCl, 19 K-Gluconate, 5 NaCl, 4 $MgCl_2$, 10 HEPES, 0.1 EGTA, 4 Mg-ATP, $Na_2$-GTP (pH: 7.3–7.4; osmolarity: 280–290 mOsm). Data were collected using a MultiClamp 700B amplifier (Molecular Devices, Sunnyvale CA). Signals were filtered at 2 kHz and digitized at 10 kHz with a Digidata 1550 Data Acquisition System, and analyzed using pCLAMP 10 software (Molecular Devices) or Mini Analysis 6.0.3 (Synaptosoft, Decatur GA).

For field potential recording in somatosensory cortex in awake mice, a specialized recording headplate was adhered to the mouse two weeks prior to recording. Following 3 days of training on the treadmill platform, a craniotomy was made above the somatosensory cortex under general anesthesia, as described above, except that a smaller glass coverslip (2 mm diameter) was affixed over part of the craniotomy to provide an unobstructed region for micropipette insertion and recording (Supplementary Fig. 2e). After recovery from the surgery, mice were head-fixed and allowed to move on the treadmill. A glass pipettes filled with ACSF containing Alexa-594 was inserted through the dura and into the cortex under two-photon guidance. Data were acquired continuously in the awake and anesthetized conditions using the parameters described above for single-cell recording.

**Two-photon Imaging of Acute Brain Slices—**Transverse brain slices were used for microglial imaging. The preparation of acute brain slices is the same as described above in Electrophysiology. The imaging protocol is the same as described above in *in vivo* Two-Photon Imaging, except with modified imaging stack parameters (100–140 μm depth, 2 μm-step size). Data analyses from slice imaging is the same as *in vivo*. Drugs were bath applied. To prepare isoflurane-enriched ACSF, carbogen gas was passed through an Anesthetic Vaporizer (Midmark Matrix VIP 3000, OH, USA) at a constant flow rate of 500 ml/min and then bubbled through the ACSF reservoir.

Author Manuscript Author Manuscript Author Manuscript Author Manuscript

**RNAscope *In situ* Hybridization and Immunohistofluorescence Staining—**To visualize β2 adrenergic receptor (Adrb2) mRNA in situ, the RNAscope® 2.5 HD Detection Kit (#322360, Advanced Cell Diagnostics, CA, USA) was applied in accordance with the manufacturer's protocol using fixed, frozen sections of 10 μm thickness. Briefly, sections were first dried for 30 min at 60°C and cleared of OCT by a 5-min phosphate-buffered saline (PBS) wash. During pretreatment, the sections were incubated in hydrogen peroxide for 10 min at RT. Then the slides were submerged into 1x target retrieval solution for 5 min at 98–102 °C. After antigen retrieval, the slides were immediately transferred to distilled water and rinsed 3–5 times. Wash steps were then repeated with 100% EtOH. The sections were then incubated in Protease Plus for protein digestion at 40 °C, 30 min. To run the assay, the RNAscope® Probe Mm-Adrb2 (#449771) was applied on pre-treated sections for 120 min at 40 °C. After probe hybridization, the signal was amplified by incubation with amplifier 1–6 in sequence. Each incubation step was followed by two 2 min washes using washing buffer. To visualize hybridized signal, 2.5 HD Detection Reagent -RED (#322360) was applied on the sections for 10min at RT. The sections were rinsed in fresh tap water before observation. To further determine expression of ADRB2 in microglia, the assay was continued with a modified immunofluorescence staining protocol following the manufacturer's instructions. Florescent images were acquired using a confocal microscope (Zeiss LSM-810). Iba1 (Wako # 019–19741, 1:500 dilution) positive cells colocalized with two or more mRNA puncta were counted as positive.

**Statistical Analyses—**Statistical analyses utilized a paired t-test design with a two-tailed test of significance for changes within a cell across conditions. Comparisons between genotypes utilized an unpaired t-test design with a two-tailed test of significance. D'Agostino-Pearson tests were used to assess normality prior to applying a parametric or non-parametric t-test variant (paired: Wilcoxon matched-pairs rank test; unpaired: Mann-Whitney test). One-way ANOVA was used to compare three groups. All statistical testing was performed in GraphPad Prism (GraphPad Software, CA, USA). Data distribution was assumed to be normal, but this was not formally tested. Data are shown as individual values or expressed as the mean ± SEM when grouped. A $P$ value <0.05 was considered statistically significant. All the $P$ values no less than 0.0001 were provided as exact value, otherwise indicated as "$P$<0.0001". No statistical methods were used to pre-determine sample sizes but our sample sizes are similar to those reported in previous publications[13,14].

Please see the Life Sciences Reporting Summary for information about reproducibility of our work.

### Data Availability

Source data for all graphs are available from the corresponding authors upon request.

## Supplementary Material

Refer to Web version on PubMed Central for supplementary material.

Author Manuscript Author Manuscript Author Manuscript Author Manuscript

## Acknowledgements:

This work is supported by National Institutes of Health (R01NS088627, R21DE025689, R01NS112144) to L.J.W., and by a postdoctoral fellowship from the Mayo Clinic Center for Multiple Sclerosis and Autoimmune Neurology to T.C. We thank Dr. Mark Mattson (National Institute on Aging) for critical reading of the paper and members of Wu lab at Mayo for insightful discussions.

## References

1. Ransohoff RM & Perry VH Microglial physiology: unique stimuli, specialized responses. Annual review of immunology 27, 119–145 (2009).
2. Wolf SA, Boddeke HW & Kettenmann H Microglia in Physiology and Disease. Annu Rev Physiol 79, 619–643 (2017). [PubMed: 27959620]
3. Kettenmann H, Hanisch UK, Noda M & Verkhratsky A Physiology of microglia. Physiol Rev 91, 461–553 (2011). [PubMed: 21527731]
4. Wu Y, Dissing-Olesen L, MacVicar BA & Stevens B Microglia: Dynamic Mediators of Synapse Development and Plasticity. Trends Immunol 36, 605–613 (2015). [PubMed: 26431938]
5. Eyo UB & Wu LJ Bi-directional microglia-neuron communication in the healthy brain. Neural plasticity 2013, 456857 (2013). [PubMed: 24078884]
6. Salter MW & Stevens B Microglia emerge as central players in brain disease. Nat Med 23, 1018–1027 (2017). [PubMed: 28886007]
7. Miyamoto A, et al. Microglia contact induces synapse formation in developing somatosensory cortex. Nat Commun 7, 12540 (2016). [PubMed: 27558646]
8. Weinhard L, et al. Microglia remodel synapses by presynaptic trogocytosis and spine head filopodia induction. Nat Commun 9, 1228 (2018). [PubMed: 29581545]
9. Tremblay ME, Lowery RL & Majewska AK Microglial interactions with synapses are modulated by visual experience. PLoS Biol 8, e1000527 (2010). [PubMed: 21072242]
10. Schafer D, et al. Microglia sculpt postnatal neural circuits in an activity and complement-dependent manner. Neuron (2012).
11. Parkhurst CN, et al. Microglia promote learning-dependent synapse formation through brain-derived neurotrophic factor. Cell 155, 1596–1609 (2013). [PubMed: 24360280]
12. Akiyoshi R, et al. Microglia Enhance Synapse Activity to Promote Local Network Synchronization. eNeuro 5 (2018).
13. Nimmerjahn A, Kirchhoff F & Helmchen F Resting microglial cells are highly dynamic surveillants of brain parenchyma in vivo. Science 308, 1314–1318 (2005). [PubMed: 15831717]
14. Davalos D, et al. ATP mediates rapid microglial response to local brain injury in vivo. Nat Neurosci 8, 752–758 (2005). [PubMed: 15895084]
15. Eyo UB, et al. P2Y12R-Dependent Translocation Mechanisms Gate the Changing Microglial Landscape. Cell Rep 23, 959–966 (2018). [PubMed: 29694903]
16. Haynes SE, et al. The P2Y(12) receptor regulates microglial activation by extracellular nucleotides. Nat Neurosci 9, 1512–1519 (2006). [PubMed: 17115040]
17. Wu LJ, Vadakkan KI & Zhuo M ATP-induced chemotaxis of microglial processes requires P2Y receptor-activated initiation of outward potassium currents. Glia 55, 810–821 (2007). [PubMed: 17357150]
18. Wake H, Moorhouse AJ, Jinno S, Kohsaka S & Nabekura J Resting microglia directly monitor the functional state of synapses in vivo and determine the fate of ischemic terminals. J Neurosci 29, 3974–3980 (2009). [PubMed: 19339593]
19. Eyo UB, et al. Regulation of Physical Microglia-Neuron Interactions by Fractalkine Signaling after Status Epilepticus. eNeuro 3 (2017).
20. Eyo UB, et al. Neuronal hyperactivity recruits microglial processes via neuronal NMDA receptors and microglial P2Y12 receptors after status epilepticus. J Neurosci 34, 10528–10540 (2014). [PubMed: 25100587]

Author Manuscript Author Manuscript Author Manuscript Author Manuscript


21. Madry C, et al. Microglial Ramification, Surveillance, and Interleukin-1beta Release Are Regulated by the Two-Pore Domain K(+) Channel THIK-1. Neuron 97, 299–312 e296 (2018). [PubMed: 29290552]
22. Franks NP General anaesthesia: from molecular targets to neuronal pathways of sleep and arousal. Nat Rev Neurosci 9, 370–386 (2008). [PubMed: 18425091]
23. Petersen CC The functional organization of the barrel cortex. Neuron 56, 339–355 (2007). [PubMed: 17964250]
24. Zhao S, et al. Cell type-specific channelrhodopsin-2 transgenic mice for optogenetic dissection of neural circuitry function. Nat Methods 8, 745–752 (2011). [PubMed: 21985008]
25. Eyo UB, Murugan M & Wu LJ Microglia-Neuron Communication in Epilepsy. Glia 65, 5–18 (2017). [PubMed: 27189853]
26. Dissing-Olesen L, et al. Activation of neuronal NMDA receptors triggers transient ATP-mediated microglial process outgrowth. J Neurosci 34, 10511–10527 (2014). [PubMed: 25100586]
27. Liang KJ, et al. Regulation of dynamic behavior of retinal microglia by CX3CR1 signaling. Investigative ophthalmology & visual science 50, 4444–4451 (2009). [PubMed: 19443728]
28. Eyo UB, et al. Regulation of Physical Microglia-Neuron Interactions by Fractalkine Signaling after Status Epilepticus. eNeuro 3 (2016).
29. Wu LJ & Zhuo M Resting microglial motility is independent of synaptic plasticity in mammalian brain. J Neurophysiol 99, 2026–2032 (2008). [PubMed: 18256162]
30. Muller CP, et al. The in vivo neurochemistry of the brain during general anesthesia. J Neurochem 119, 419–446 (2011). [PubMed: 21883214]
31. Zhang Y, et al. An RNA-sequencing transcriptome and splicing database of glia, neurons, and vascular cells of the cerebral cortex. J Neurosci 34, 11929–11947 (2014). [PubMed: 25186741]
32. Gyoneva S & Traynelis SF Norepinephrine modulates the motility of resting and activated microglia via different adrenergic receptors. J Biol Chem 288, 15291–15302 (2013). [PubMed: 23548902]
33. Schwarz LA & Luo L Organization of the locus coeruleus-norepinephrine system. Curr Biol 25, R1051–R1056 (2015). [PubMed: 26528750]
34. Sipe GO, et al. Microglial P2Y12 is necessary for synaptic plasticity in mouse visual cortex. Nat Commun 7, 10905 (2016). [PubMed: 26948129]
35. Berridge CW & Waterhouse BD The locus coeruleus-noradrenergic system: modulation of behavioral state and state-dependent cognitive processes. Brain Res Brain Res Rev 42, 33–84 (2003). [PubMed: 12668290]
36. Audet MA, Doucet G, Oleskevich S & Descarries L Quantified regional and laminar distribution of the noradrenaline innervation in the anterior half of the adult rat cerebral cortex. J Comp Neurol 274, 307–318 (1988). [PubMed: 2464617]
37. O'Donnell J, Zeppenfeld D, McConnell E, Pena S & Nedergaard M Norepinephrine: a neuromodulator that boosts the function of multiple cell types to optimize CNS performance. Neurochem Res 37, 2496–2512 (2012). [PubMed: 22717696]
38. Kohm AP & Sanders VM Norepinephrine and beta 2-adrenergic receptor stimulation regulate CD4+ T and B lymphocyte function in vitro and in vivo. Pharmacol Rev 53, 487–525 (2001). [PubMed: 11734616]
39. Orr AG, Orr AL, Li XJ, Gross RE & Traynelis SF Adenosine A(2A) receptor mediates microglial process retraction. Nat Neurosci 12, 872–878 (2009). [PubMed: 19525944]
40. Bernier LP, et al. Nanoscale Surveillance of the Brain by Microglia via cAMP-Regulated Filopodia. Cell reports 27, 2895–2908 e2894 (2019). [PubMed: 31167136]
41. Eyo UB, et al. Modulation of microglial process convergence toward neuronal dendrites by extracellular calcium. J Neurosci 35, 2417–2422 (2015). [PubMed: 25673836]
42. Zhao X, Eyo UB, Murugan M & Wu LJ Microglial interactions with the neurovascular system in physiology and pathology. Dev Neurobiol 78, 604–617 (2018). [PubMed: 29318762]
43. Li Y, Du XF, Liu CS, Wen ZL & Du JL Reciprocal regulation between resting microglial dynamics and neuronal activity in vivo. Dev Cell 23, 1189–1202 (2012). [PubMed: 23201120]

Author Manuscript Author Manuscript Author Manuscript Author Manuscript

44. Chan-Palay V & Asan E Alterations in catecholamine neurons of the locus coeruleus in senile dementia of the Alzheimer type and in Parkinson's disease with and without dementia and depression. J Comp Neurol 287, 373–392 (1989). [PubMed: 2570794]

45. Kvetnansky R, Sabban EL & Palkovits M Catecholaminergic systems in stress: structural and molecular genetic approaches. Physiol Rev 89, 535–606 (2009). [PubMed: 19342614]

46. Heneka MT, et al. Locus ceruleus controls Alzheimer's disease pathology by modulating microglial functions through norepinephrine. Proc Natl Acad Sci U S A 107, 6058–6063 (2010). [PubMed: 20231476]

47. Xu H, Rajsombath MM, Weikop P & Selkoe DJ Enriched environment enhances beta-adrenergic signaling to prevent microglia inflammation by amyloid-beta. EMBO Mol Med 10 (2018).

48. Hong S, et al. Complement and microglia mediate early synapse loss in Alzheimer mouse models. Science 352, 712–716 (2016). [PubMed: 27033548]

49. Mitchell HA & Weinshenker D Good night and good luck: norepinephrine in sleep pharmacology. Biochem Pharmacol 79, 801–809 (2010). [PubMed: 19833104]

50. Brown EN, Lydic R & Schiff ND General anesthesia, sleep, and coma. N Engl J Med 363, 2638–2650 (2010). [PubMed: 21190458]

51. Jung S, et al. Analysis of fractalkine receptor CX(3)CR1 function by targeted deletion and green fluorescent protein reporter gene insertion. Mol Cell Biol 20, 4106–4114 (2000). [PubMed: 10805752]

52. Schindelin J, et al. Fiji: an open-source platform for biological-image analysis. Nature methods 9, 676–682 (2012). [PubMed: 22743772]

Author Manuscript Author Manuscript Author Manuscript Author Manuscript

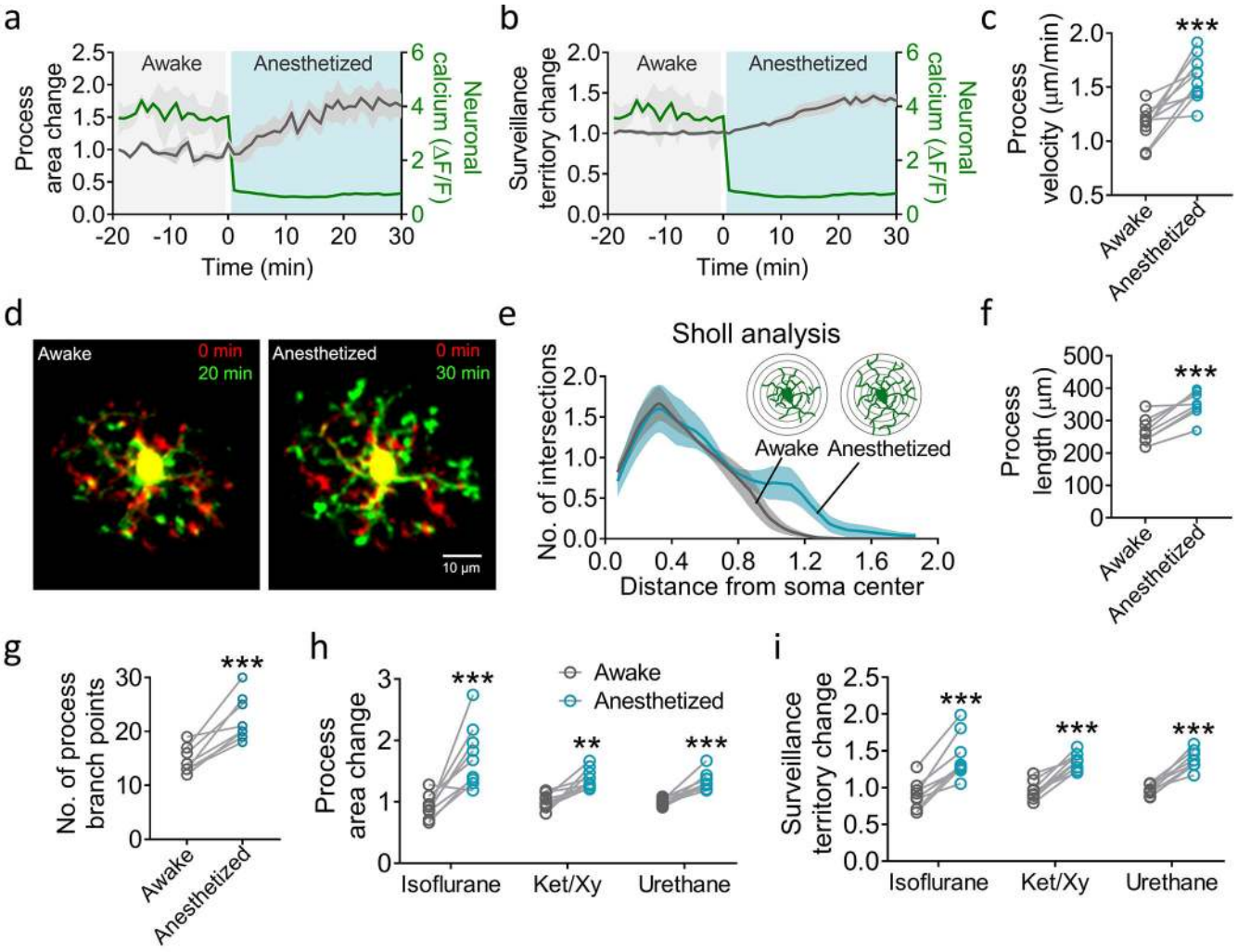


**Fig. 1: Microglial process surveillance is increased after general anesthesia.**

**a-b**, Time-lapse changes in microglial process area (**a**) and surveillance territory (**b**) overlaid with corresponding changes in neuronal calcium activity as the animal transitions from an awake to an anesthetized state. Isoflurane was used for anesthesia induction and maintenance (**a-g**). **c**, Process velocity changes under awake and anesthetized conditions ($n$=12 cells/3 mice, $P$<0.0001, t(11)=6.031). **d**, Representative images of microglial morphology changes over a 20 min period (red, 0 min; green, 20 min) during the awake condition and under isoflurane anesthesia. **e-g**, Sholl analysis of microglial morphology (**e**), along with changes in microglial process length (**f**) ($P$=0.0002, t(8)=6.302) and process branch points (**g**) ($P$=0.0003, t(8)=6.22) before and after anesthesia. **h**,**i**, Microglial process area (**h**) (Isoflurane: $P$=0.0003, t(8)=4.647; Ket/Xy: $P$=0.0011, t(8)=4.969; Urethane: $P$=0.0001, t(8)=6.763) and surveillance territory (**i**) (Isoflurane: $P$=0.0001, t(8)=7.093; Ket/Xy: $P$=0.0001, t(8)=9.134; Urethane: $P$=0.0001, t(8)=9.102) changes induced by different anesthetic agents: isoflurane, ketamine/xylazine (Ket/Xy), and urethane compared to the awake baseline period. $N$=9 cells/3 mice for each group, $^{**}P \leq 0.01$, $^{***}P \leq 0.001$, paired t-test (two-tailed), unless otherwise indicated. Trend lines display the mean ± SEM

change in (**a**,**b**,**e**). Experiments were repeated three times independently with similar results in (**d**).

Author Manuscript Author Manuscript Author Manuscript Author Manuscript

Author Manuscript Author Manuscript Author Manuscript Author Manuscript

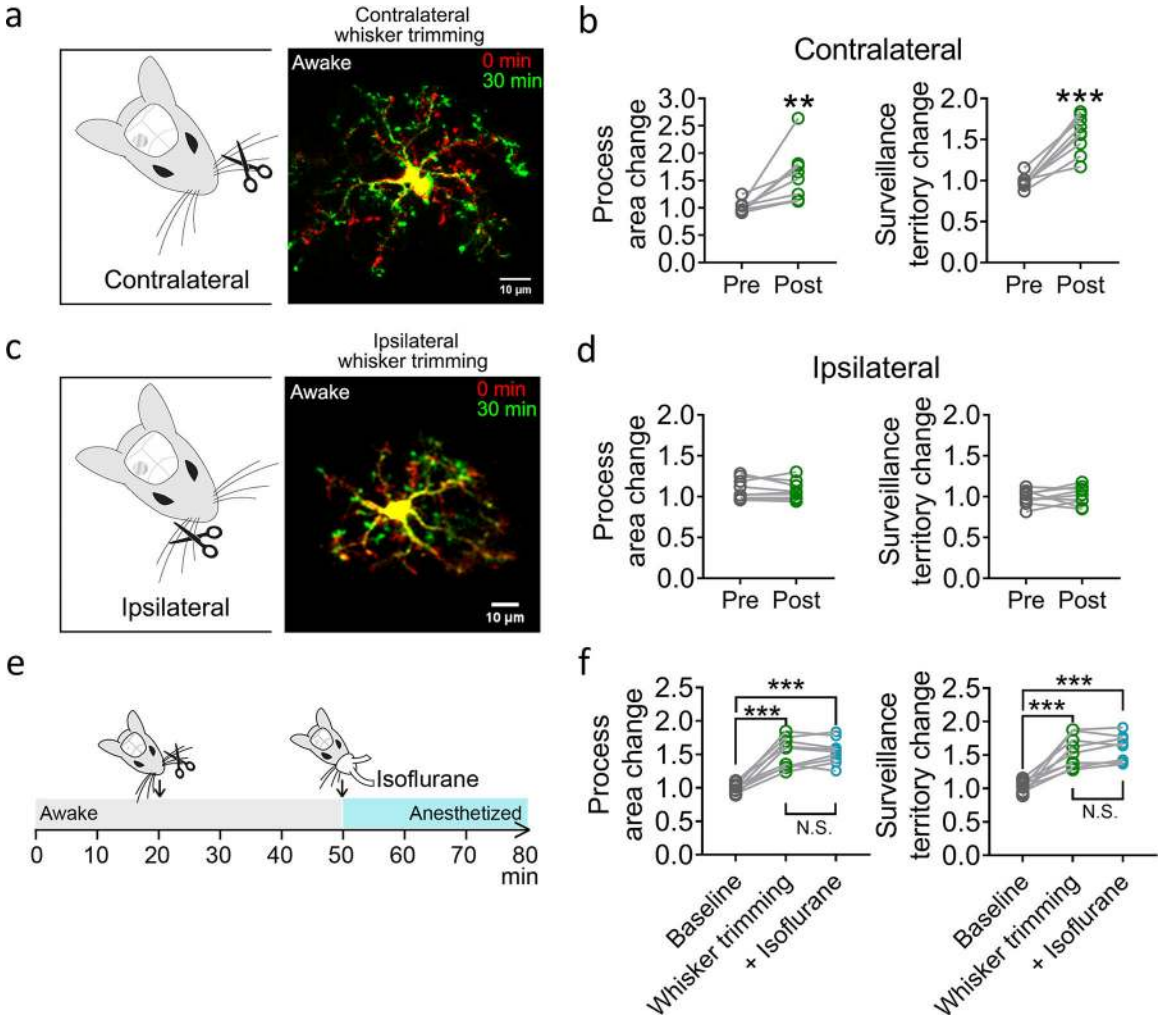


**Fig. 2: Whisker trimming increases microglial process surveillance in the barrel cortex of awake mice.**

**a**, Microglial morphology in the contralateral barrel cortex before (red) and 30 min after (green) whisker trimming in awake mice. **b**, Increased microglial process area and surveillance territory after trimming the contralateral whiskers (area: $P$=0.0079, t(8)=3.512; territory: $P$=0.0001, t(8)=8.152). **c**, Microglial morphology in the ipsilateral barrel cortex before (red) and 30 min after (green) whisker trimming in awake mice. **d**, No observed changes in microglial process area and surveillance territory after trimming the ipsilateral whiskers (area: $P$=0.5439, t(8)=0.63337; territory: $P$=0.5086, t(8)=0.6919). **e**, Experimental paradigm: microglial process dynamics were studied in the awake mouse at baseline before trimming the contralateral whiskers 20 min later. In addition, isoflurane was then introduced 30 min after whisker trimming. **f**, Microglial process area and surveillance increase in the contralateral barrel cortex following trimming but do not show an additional increase when isoflurane is later administered (area: whisker trimming vs baseline, $P$<0.0001, t(8)=7.34; +Isoflurane vs baseline, $P$<0.0001, t(8)=9.153; whisker trimming vs +Isoflurane, $P$=0.624, t(8)=0.5097; territory: whisker trimming vs baseline, $P$=0.0004, t(8)=5.89; +Isoflurane vs baseline, $P$=0.0002, t(8)=6.639; whisker trimming vs +Isoflurane, $P$=0.2184, t(8)=1.336).

Author Manuscript Author Manuscript Author Manuscript Author Manuscript

$N$=9 cells/3 mice for each group, $^{**}P \leq 0.01$, $^{***}P \leq 0.001$, paired t-test (two-tailed). Experiments were repeated three times independently with similar results in (**a**,**c**).

Author Manuscript Author Manuscript Author Manuscript Author Manuscript

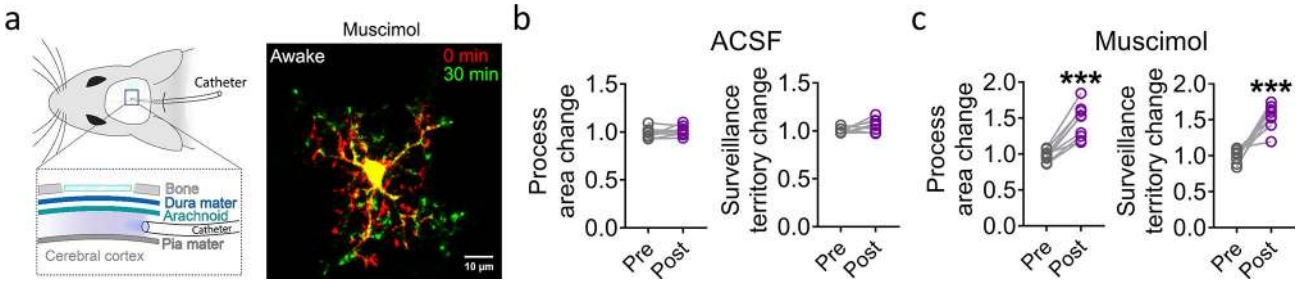


**Fig. 3: Intracerebral application of muscimol increases microglial process surveillance.**

**a**, Placement of a drug infusion catheter in the subarachnoid space adjacent to the area of cranial window imaging. Imaging of microglia before (red) and 30 min after (green) intracerebral administration of muscimol (870 μM). **b**-**c**, Changes in microglial process area and surveillance territory before and after administration of ACSF (**b**) (area: $P$=0.2681, t(8)=1.19; territory: $P$=0.0911, t(8)=1.92) or muscimol (**c**) (area: $P$<0.0001, t(8)=7.338; territory: $P$<0.0001, t(8)=7.386). $N$=9 cells/3 mice for each group, ***$P \leq 0.001$, paired t-test (two-tailed). Experiments were repeated three times independently with similar results in (**a**).

Author Manuscript Author Manuscript Author Manuscript Author Manuscript

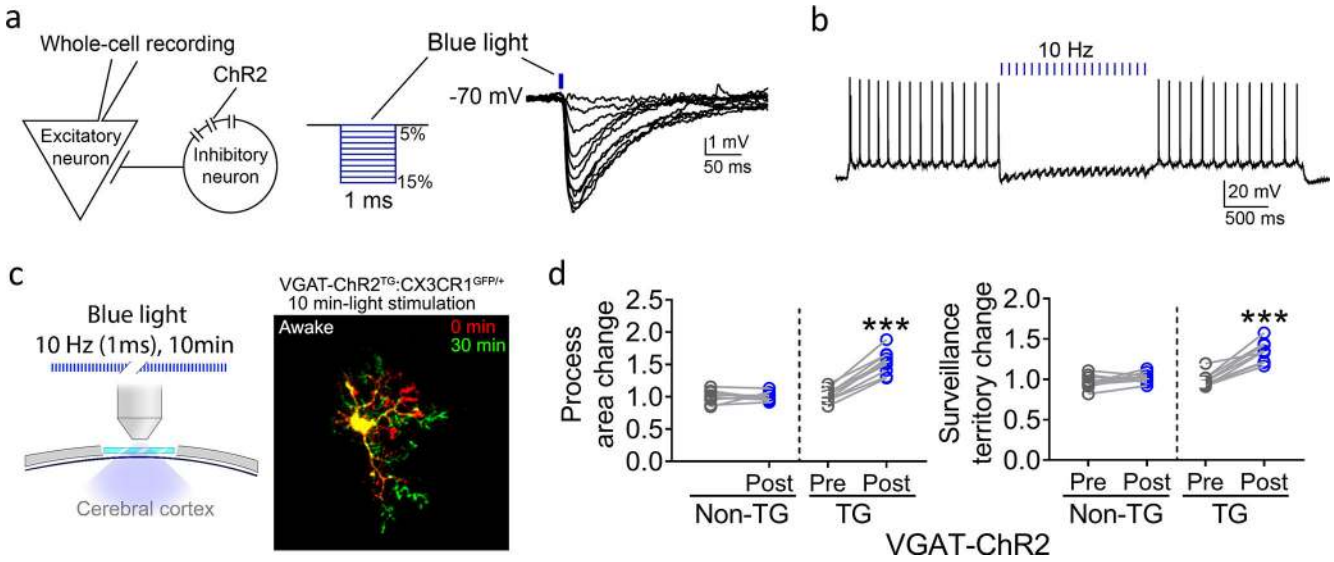


**Fig. 4: Optogenetic suppression of neuronal activity through VGAT-ChR2 mediated inhibition increases microglial process surveillance.**

**a**, Whole-cell recording of an excitatory neuron (identified by firing pattern and morphology) adjacent to an inhibitory interneuron expressing ChR2 in a brain slice. A blue light pulse (1 ms, 470 nm) induced intensity-dependent (5%−15%) membrane hyperpolarization in the neuron, recorded in current-clamp mode. **b**, A 10 Hz train of blue light pulses inhibits local excitatory neuron firing in real time. **c**, *In vivo* experimental paradigm for inducing on-demand inhibition in the somatosensory cortex (470 nm light, 10 Hz train, 1 ms pulse, 10 min). Representative image of microglial morphology prior to (red) and following (green) 10 min light stimulation. **d**, Changes in microglial process area (Non-TG: $P$=0.7144, t(8)=0.3793; TG: $P$<0.0001, t(8)=12.67) and surveillance territory (Non-TG: $P$=0.1140, t(8)=1.774; TG: $P$<0.0001, t(8)=8.051) before and after light stimulation in animals that express the VGAT-ChR2 transgene ("TG") or their non-transgenic sibling littermates ("non-TG"). $N$=9 cells/3 mice for each group, ***$P \leq 0.001$, paired t-test (two-tailed). Experiments were repeated three times independently with similar results in (**a**,**b**,**c**).

Author Manuscript Author Manuscript Author Manuscript Author Manuscript

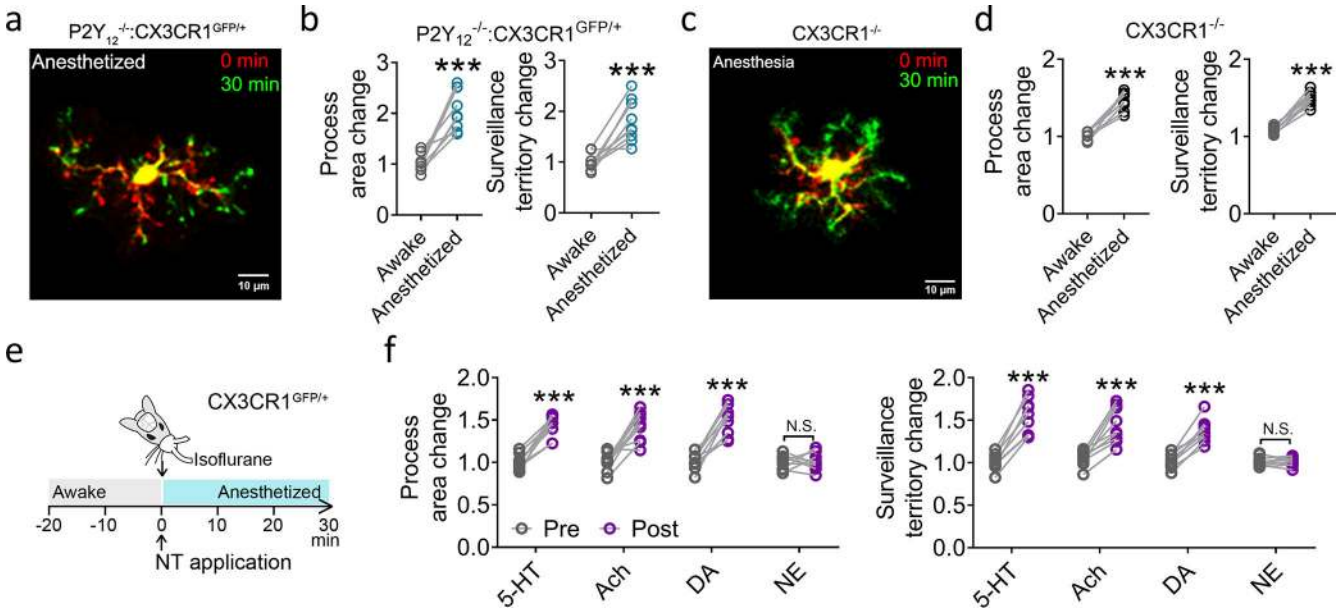


**Fig. 5: Norepinephrine signaling, but not $P2Y_{12}$ or CX3CR1 signaling, contributes to microglial surveillance increases.**

**a**, Representative image of $P2Y_{12}^{-/-}$ microglial morphology prior to (red) and following (green) isoflurane anesthesia. **b**, The previously reported increases in microglial process area and surveillance territory following isoflurane anesthesia were not prevented by $P2Y_{12}^{-/-}$ (area: $P<0.0001$, t(8)=7.4; territory: $P=0.0007$, t(8)=5.306). **c**, Representative image of $CX3CR1^{-/-}$ microglial morphology prior to (red) and following (green) isoflurane anesthesia. **d**, The previously reported increases in microglial process area and surveillance territory following isoflurane anesthesia were not prevented by $CX3CR1^{-/-}$ (area: $P<0.0001$, t(8)=10.13; territory: $P<0.0001$, t(8)=13.76). **e**, Experimental paradigm used to test the effects of different candidate neurotransmitters on microglial process dynamics during isoflurane anesthesia. **f**, Changes of microglial process area and surveillance territory in response to isoflurane anesthesia were not affected by intracerebral administration of acetylcholine (Ach, area: $P=0.0005$, t(8)=5.584; territory: $P=0.0003$, t(8)=6.084), dopamine (DA, area: $P<0.0001$, t(8)=7.538; territory: $P<0.0001$, t(8)=8.586), or serotonin (5-HT, area: $P<0.0001$, t(8)=8.995; territory: $P<0.0001$, t(8)=9.944). However, intracerebral administration of norepinephrine (NE) prevented the observed increases in microglial process area and surveillance territory following isoflurane anesthesia (area: $P=0.9346$, t(8)=0.08465; territory: $P=0.7332$, t(8)=0.3531). $N=9$ cells/3 mice for each group, $^{***}P \leq 0.001$, paired t-test (two-tailed). Experiments were repeated three times independently with similar results in (**a**,**c**).

Author Manuscript Author Manuscript Author Manuscript Author Manuscript

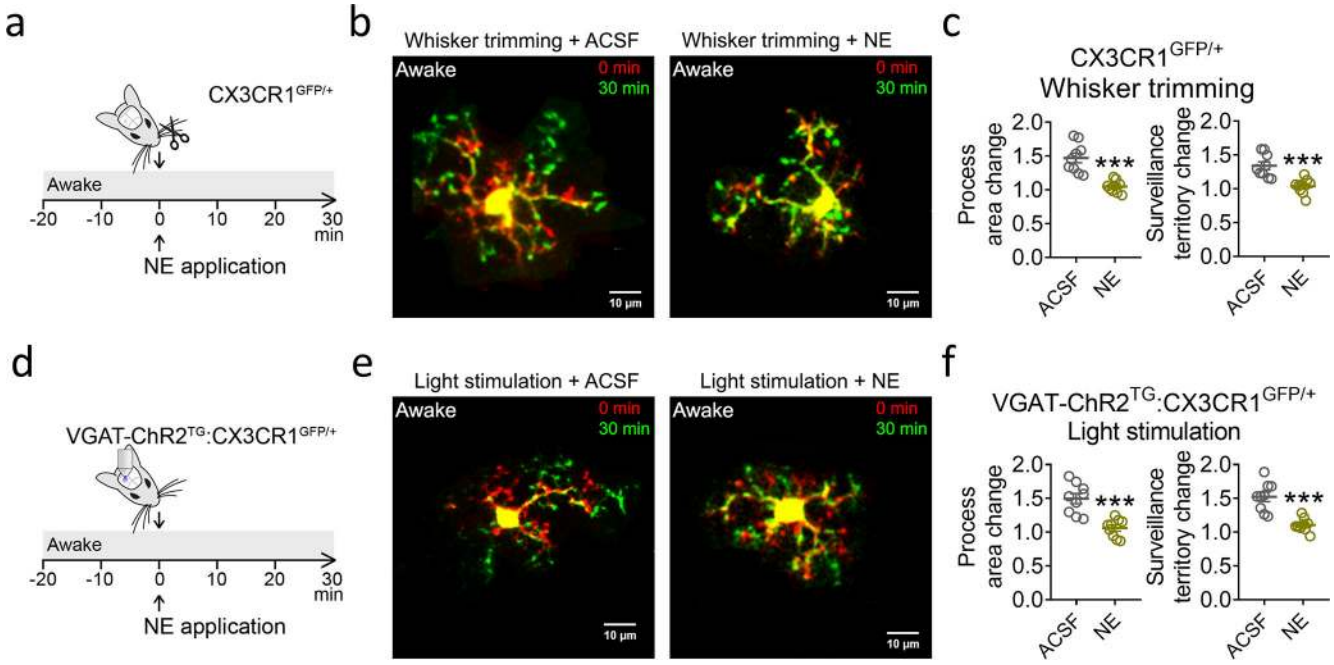


**Fig. 6: Norepinephrine administration prior to whisker trimming or optogenetic inhibition prevents the increase in microglial process surveillance**

**a**, Experimental paradigm: NE (or ACSF control solution) is administered intracerebrally just prior to contralateral whisker trimming. **b**, Representative images of microglial morphology prior to (red) and following (green) whisker trimming, with either ACSF or NE applied. **c**, NE, but not ACSF, prevents changes in microglial process area (ACSF: 1.473±0.072; NE: 1.048±0.030) and surveillance territory (ACSF: 1.341±0.058; NE: 1.038±0.037) induced by contralateral whisker trimming (area: $P<0.0001$, t(16)=5.432; territory: $P=0.0005$, t(16)=4.395). **d**, Experimental paradigm: NE (or ACSF control solution) is administered intracerebrally just prior to optogenetic stimulation of VGAT-ChR2 transgenic mice. **e**, Representative images of microglial morphology prior to (red) and following (green) optogenetic inhibition, with either ACSF of NE applied just prior to light stimulation. **f**, NE, but not ACSF, also prevents changes in microglial process area (ACSF: 1.496±0.075; NE: 1.060±0.045) and surveillance territory (ACSF: 1.523±0.070; NE: 1.106±0.033) induced by optogenetic inhibition (area: $P=0.0001$, t(16)=5; territory: $P<0.0001$, t(16)=5.334). $N=9$ cells/3 mice for each group, $^{***}P \leq 0.001$, unpaired t-test (two-tailed). Experiments were repeated three times independently with similar results in (**b**,**e**).

Author Manuscript Author Manuscript Author Manuscript Author Manuscript

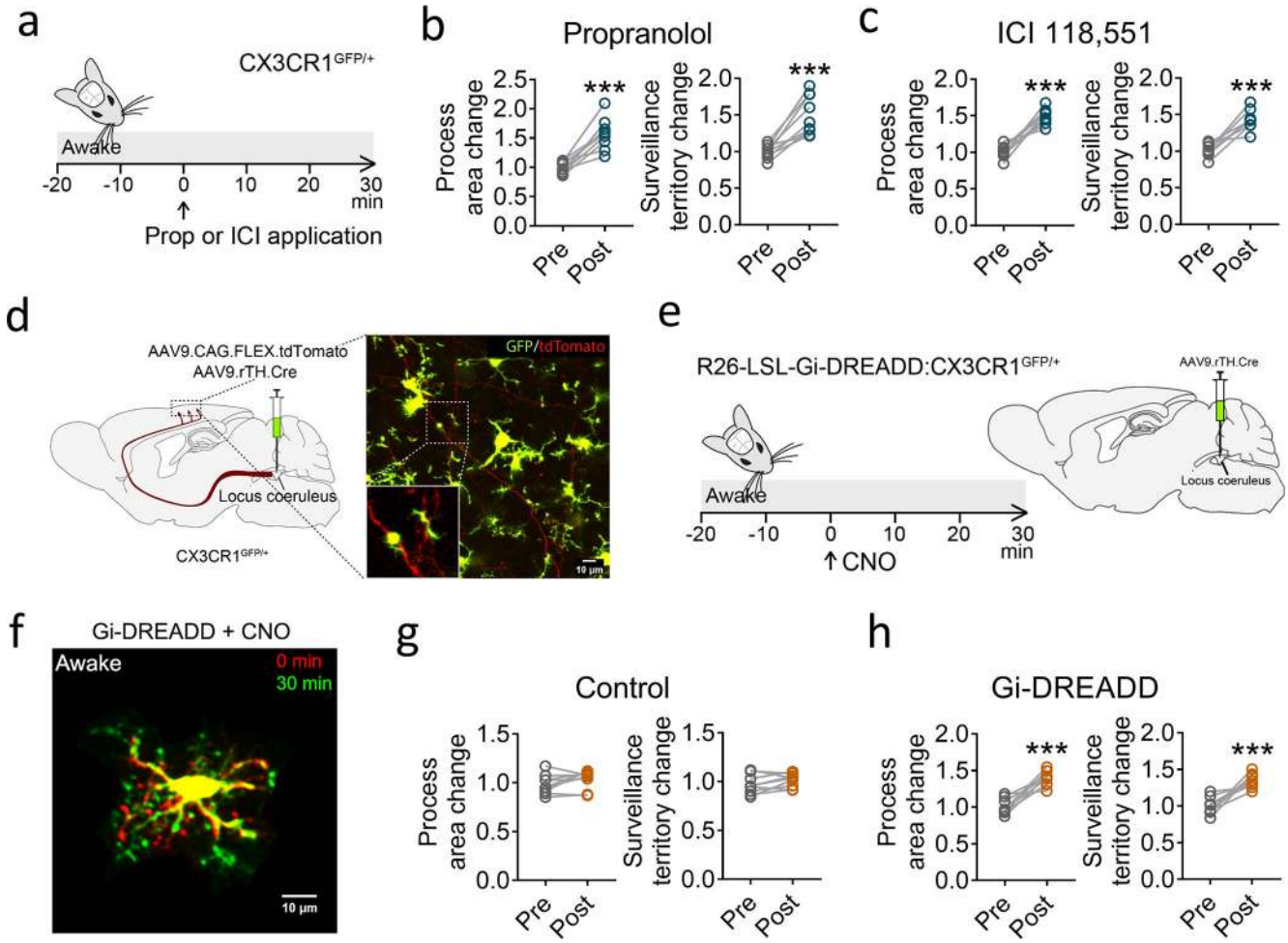


**Fig. 7: Blocking adrenergic receptors or lowering endogenous norepinephrine signaling increases microglial process surveillance**

**a**, Experimental paradigm: The β1/2 receptor antagonist propranolol (prop) or β2 receptor antagonist ICI 118,551 (ICI) are administered intracerebrally in awake mice. **b-c**, Both propranolol (**b**) (area: $P$=0.0002, t(8)=6.331; territory: $P$=0.0003, t(8)=6.204) and ICI 118,551 (**c**) (area: $P$<0.0001, t(8)=9.024; territory: $P$=0.0001, t(8)=7.109) infusion in awake mice can trigger an increase in microglial process area and territory surveillance. **d**, To determine the extent of noradrenergic innervation in the somatosensory cortex by LC neurons, td-Tomato expression was induced selectively in LC neurons using a specific Cre recombination strategy in CX3CR1$^{GFP/+}$ mice. The fluorescent micrograph shows heavy noradrenergic innervation of the somatosensory cortex by LC projections. **e**, Experimental paradigm: The DREADD receptor agonist CNO is administered (i.p.) to Gi DREADD mice and control sibling littermates. **f**, Representative images of microglial morphology prior to (red) and following (green) CNO administration in a Gi DREADD mouse. **g-h**, CNO administration in control mice (**g**) does not alter microglial process area or territory surveillance (area: $P$=0.1193, t(8)=1.744; territory: $P$=0.1326, t(8)=1.674), while CNO administration in Gi-DREADD mice (**h**) increases microglial process area and territory surveillance (area: $P$=0.0001, t(8)=6.815; territory: $P$=0.0005, t(8)=5.67). $N$=9 cells/3 mice

Author Manuscript Author Manuscript Author Manuscript Author Manuscript

for each group, ***$P \leq 0.001$, paired t-test (two-tailed). Experiments were repeated three times independently with similar results in (**d**,**f**).

Author Manuscript Author Manuscript Author Manuscript Author Manuscript

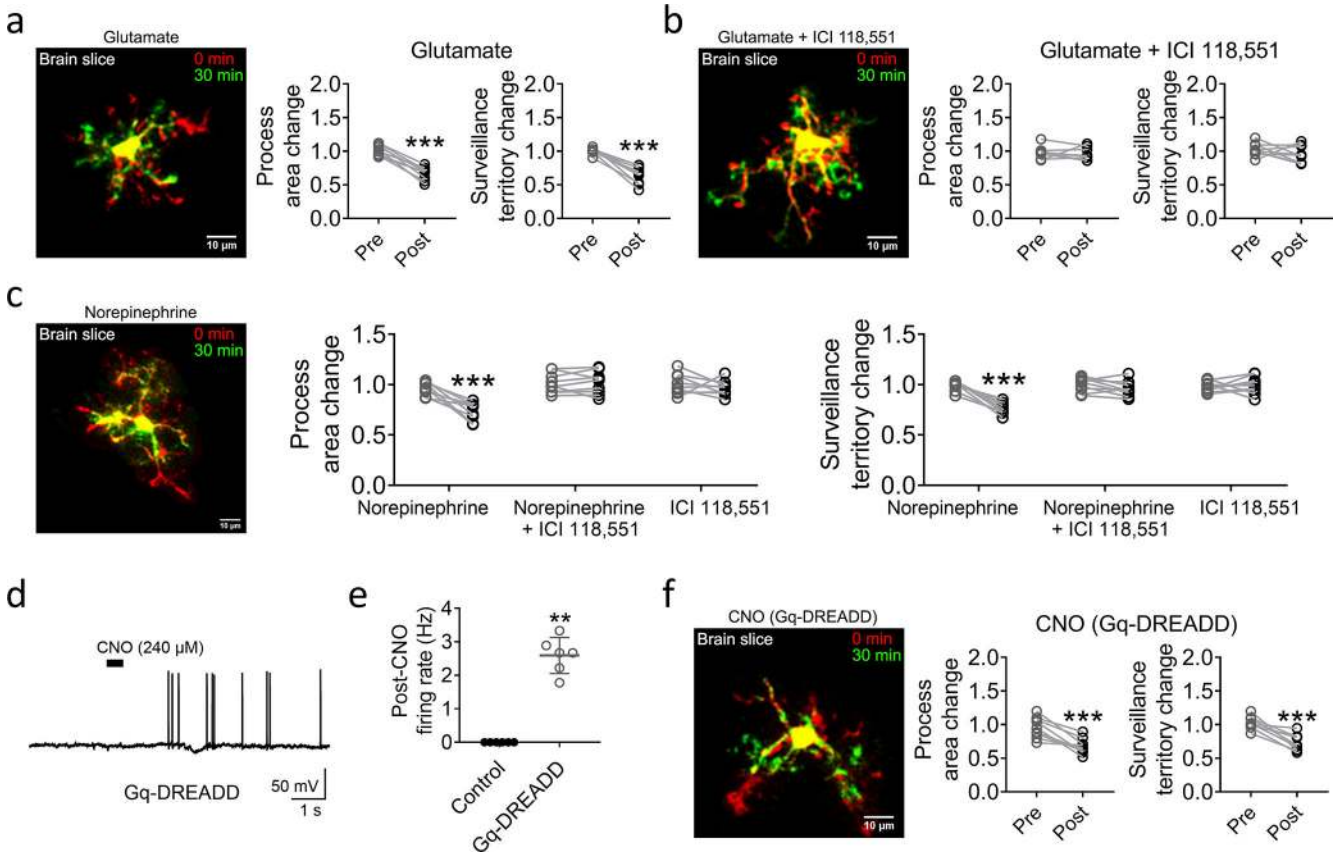


**Fig. 8: Norepinephrine decreases microglial process surveillance in acute brain slices**

**a**,**b**, Microglial morphology changes in acute brain slices before (red) and 30 min after (green) bath application of 50 μM glutamate (**a**) (area: $P<0.0001$, t(8)=9.982; territory: $P<0.0001$, t(8)=8.027), or 50 μM glutamate with 10 μM ICI 118,551 (**b**) (area: $P=0.625$, t(8)=0.509; territory: $P=0.264$, t(8)=1.202). **c**, Microglial morphology changes in acute brain slices before (red) and 30 min after (green) bath application of 30 μM norepinephrine (area: $P=0.0003$, t(8)=6.127; territory: $P<0.0001$, t(8)=8.932), 30 μM norepinephrine with 10 μM ICI 118,551 (area: $P=0.859$, t(8)=0.183; territory: $P=0.137$, t(8)=1.654) or 10 μM ICI 118,551 (area: $P=0.420$, t(8)=0.850; territory: $P=0.672$, t(8)=0.440). **d**, After a delay associated with CNO bath diffusion, Gq-DREADD neurons in the LC display a marked increase in firing frequency. Experiments were repeated three times independently with similar result. **e**, Effects of CNO on firing rates are only observed in Gq-DREADD neurons in LC, but not in control neurons (Control: 0; Gq-DREADD: 593±0.219; $P=0.002$, t(10)=11.8). $N=6$ cells/3 mice for each group, $^{**}P<0.01$, unpaired t-test (two-tailed). **f**, Microglial morphology changes in acute brain slices from mice that expressed Gq-DREADD in LC before (red) and 30 min after (green) bath application of CNO (10 μM) (area: $P=0.0005$, t(8)=5.573; territory: $P=0.0004$, t(8)=5.797). $N=9$ cells/3 mice for each group, $^{***}P<0.001$, paired t-test (two tailed), unless otherwise indicated. Experiments were repeated three times independently with similar results in (**a**,**b**,**c**,**d**,**f**).